make the error in E_B as small as possible. This was accomplished by deducing the velocity from a calibration based upon grain density $\bar{g}$ *vs residual range* R, rather than from $\bar{g}$ *vs* $\bar{\alpha}$, the mean deviation due to multiple coulomb scattering. In the same stack, 48 long tracks of protons, pions, and muons arrested by ionization had been grain counted as a function of range. [For blobs, the convention was employed that the grain count=(blob length)/(mean grain diameter)]. An empirical curve was thus obtained which conforms, at least for $\bar{g}\lesssim 150$ grains/100 μ, to the power law

$$R=1.184\times 10^{9} m\bar{g}^{-2.387}, \tag{6}$$

where R is measured in microns, m in proton masses, and $\bar{g}$ in grains/100 μ. Combining Eq. (6) with the range-energy law [Eq. (1)], we get the kinetic energy

$$E=4.020\times 10^{4} m\bar{g}^{-1.356}\ (\text{Mev}), \tag{7}$$

and converting to the kinetic energy $(\gamma-1)$ in rest-mass units, we obtain

$$\gamma-1=42.8\bar{g}^{-1.356}, \tag{8}$$

where γ is the total energy in rest-mass units. (Neither g_{plateau} nor $g_{\min}$ is required in this calibration.) When $\bar{g}$ is thus empirically related to γ through the range, higher precision is attainable in energy and mass evaluation than when $\bar{g}$ is related to γ through the mean deviation $\bar{\alpha}$.

Since $\bar{g}$ for particle B was of course measured over a finite range interval, the energy deduced from Eq. (8) was range corrected back to the point of emission.

3. Direct Estimation of Fragment Mass from Multiple Scattering

In applying the constant-sagitta method of multiple Coulomb scattering to the estimation of the hyperfragment mass, we use the relation

$$m_F=(\bar{D}_p/\bar{D}_F)^{2.31}Z^{-0.36}, \tag{9}$$

where m_F is the fragment mass in units of the proton mass; D_F and D_p are the mean noise-corrected sagittae (second differences) for the fragment and for a group of calibration protons, respectively, obtained using the same cell scheme; and Z is the fragment's charge. The exponent 2.31 differs from that in some of the literature, and is based on recent range-energy relations.[14,23,24] We find that $D_p/D_F=2.34\pm(20\%)$. Hence $m_F=7.1Z^{-0.36}\pm(45\%)$, the relation given in the text.

PHYSICAL REVIEW VOLUME 100, NUMBER 5 DECEMBER 1, 1955

Λ^0-Fragment Decay in a Cloud Chamber*

J. D. SORRELS, G. H. TRILLING, AND R. B. LEIGHTON
Norman Bridge Laboratory of Physics, California Institute of Technology, Pasadena, California
(Received August 8, 1955)

The decay in flight of a heavy nuclear fragment is described. The event is most reasonably interpreted as the decay of a Λ^0 particle bound to a He^3 nucleus, and is similar to examples previously observed in nuclear emulsions. The lifetime of the excited fragment in this single example is $5.4\pm0.6\times10^{-10}$ sec, and the binding energy of the Λ^0 to He^3 is probably less than 2 Mev.

IN the 48-inch magnet cloud chambers operating in Pasadena, the event shown in Fig. 1 has been observed. This photograph contains what appears to be an ordinary Λ^0 decay into a proton (track B) and π^- meson (track C). The momenta, estimated ionizations, and derived masses of the labelled tracks are shown in Table I. The ionization and momentum of track B determine that it is probably due to a proton (mass$=1850\pm350\ m_e$), while track C could not be due to a particle as heavy as known K mesons. It is, however, consistent with either a π meson, μ meson, or electron.

If we assume that C is the track of a π meson, B and C together have the usual characteristics of Λ^0 decay.

TABLE I. Basic data on tracks of Fig. 1.

Track	Charge	Momentum Mev/c	Ionization times minimum	Mass m_e
A	...	...	15–30	...
B	+	298±31	5–10	1850±350
C	−	145.5±6	<2	<370
D	+	See Table III	15–30	...

TABLE II. Rectangular components of unit vectors.

Particle identification	Designation of tangents in Fig. 2	Unit vectors of tangents at decay point[a]
Fragment before decay	$O'A$ (or $O'A'$)	$(0.000\pm0.012)\mathbf{i}+(1.000)\mathbf{j}+(0.000\pm0.024)\mathbf{k}$
Proton	AB	$-0.3330\mathbf{i}-0.9238\mathbf{j}-0.1889\mathbf{k}$
π-Meson	AC	$+0.4808\mathbf{i}-0.8726\mathbf{j}+0.0867\mathbf{k}$
Fragment after decay	AD	$+0.0212\mathbf{i}-0.9986\mathbf{j}+0.0486\mathbf{k}$

[a] The errors in measurement of the direction cosines of AB, AC, and AD are negligible in the analysis of this event.

* Assisted by the joint program of the Office of Naval Research and U. S. Atomic Energy Commission. Reproduction in whole or in part is permitted for any purpose of the United States Government.

The measured Q value is 36.6±2.9 Mev, in good agreement with the known value of 37.0±0.5 Mev.

However, there are several unusual characteristics of this event which raise doubt that it is in fact an ordinary Λ^0 decay.

1. The only penetrating shower origin associated with this event is 5 mm above the top inside wall of the cloud chamber. Even though all tracks of more than 300-Mev/c momentum pass through this origin, it does not lie in the Λ^0 decay plane. The angle of noncoplanarity is 4.1±2.0°.

2. The line of flight of the Λ^0 determined from the momentum of the decay products misses this origin by 7±2 mm.

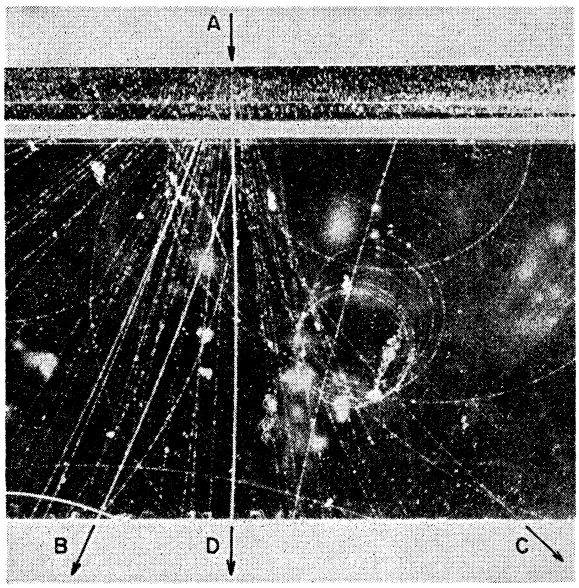

FIG. 1. A cloud-chamber photograph of a delayed fragment decay. A heavy fragment (A) is ejected from a well-defined shower origin 5 mm above the sensitive region of the chamber. The fragment subsequently decays into a proton (B), a light particle consistent with a π^- meson (C), and another secondary fragment (D). The event is consistent with the in flight decay of an excited He^4 nucleus containing a Λ^0 particle. An unrelated $\pi \rightarrow \mu + \nu$ decay appears slightly to the left of track (D).

3. The vertex of the assumed Λ^0 lies on the path of a heavy fragment (track A) ejected from the penetrating shower origin, within 0.1 mm laterally and 0.4 mm in depth.

4. There is a 3.0°±1.2° kink in the fragment track where it meets the vertex of the assumed Λ^0, whereas none of the shower tracks in the photograph shows detectable distortion.

2. The direction and magnitude of this kink are such that transverse momentum balance is possible if we assume that the fragment A undergoes a decay into B, C, and D. Table II gives the rectangular components of unit vectors oriented along the tangents to the tracks A, B, C, and D at their intersection, with respect to axes X', Y', Z' such that track A is traveling in the negative Y' direction. Figures 2, 3, and 4 show an isometric view of the four tracks; the intersection points of the tangents to tracks B, C, and D with a plane perpendicular to track A; and a transverse momentum diagram, respectively. Transverse momentum balance is excellent for a doubly charged fragment, but it is barely within experimental error for a singly charged one (Fig. 4).

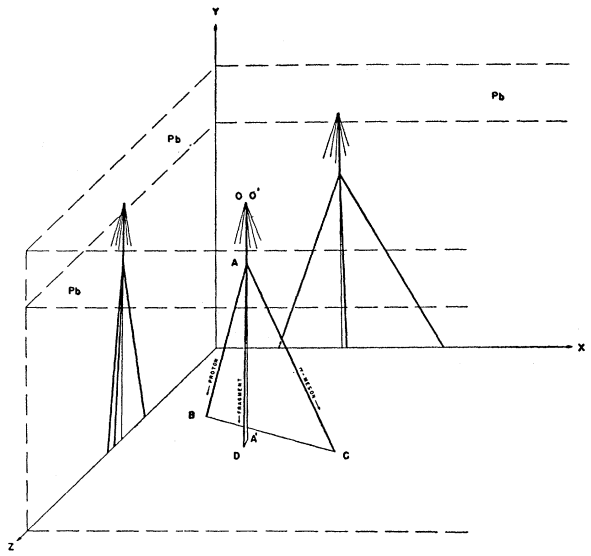

FIG. 2. An isometric view of the event shown in Fig. 1. The penetrating shower has a neutral primary for there is no track visible in the chamber above the one shown. The lines of this figure are all tangents to the pertinent tracks at the decay point (A) of the excited fragment. Thus $O'A$, the tangent to the primary fragment, does not pass exactly through O, the origin of the penetrating shower. AA' is a straight line extension of $O'A$. Orthogonal projections of the event are drawn on the back piston and a side wall.

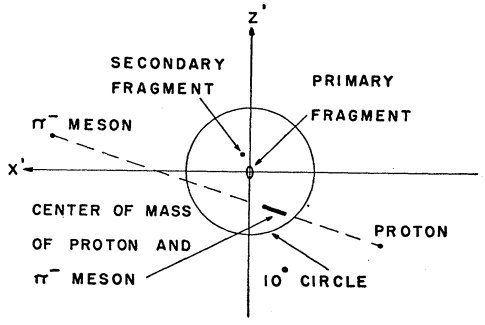

FIG. 3. The intersections of the lines of flight of the tracks of Fig. 2 with a plane transverse to the line of flight of the primary fragment. This figure shows that the sum of the transverse momenta of the proton and π^- meson is opposite in direction to the transverse momentum of the secondary fragment, within experimental error. The ellipse around the origin of the diagram represents the error in measurement of the tangent to the primary fragment at the point of decay. The errors in measurement of the directions of the secondary fragment, proton, and π meson are negligible compared to that of the primary fragment. The large circle on the diagram represents the locus of intersections made by lines which pass through Point A, Fig. 2, and make an angle of 10° to the Y' axis.

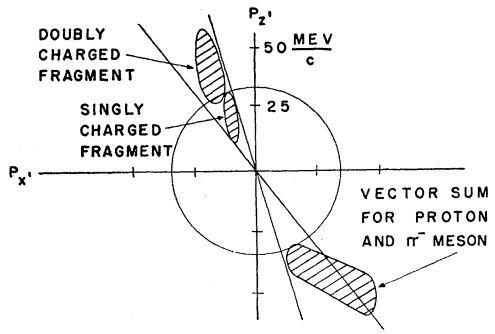

FIG. 4. Transverse momenta of the secondaries of the Λ^0 fragment decay. One region of error is drawn for the vector sum of the transverse momenta of the proton and π meson. Two other regions of error are drawn for the secondary fragment, one for a doubly charged fragment and another for a singly charged fragment. Transverse momentum balance is excellent for the doubly charged fragment.

The above characteristics strongly suggest that this event is an example of the decay of a Λ^0 particle bound to a nuclear fragment, and therefore a detailed analysis based upon this assumption has been carried out.

By comparison with the ionization of protons of known momenta, the ionization of the fragment below the kink is estimated to be within the range 15 to 30 times minimum. In Table III, the measured momenta, with errors including that due to multiple scattering, and required ionizations are listed opposite the various possible secondary fragment identities. We see that the secondary fragment is probably either H^3 or He^3, but that there is a small possibility that it is H^2 or He^4.

Therefore, if this event is an example of a Λ^0-fragment decay, it must be one of the following:

(a) $H^{3*} \leftrightarrow (\Lambda^0+H^2) \rightarrow H^2+p+\pi^-+Q_a$,

(b) $H^{4*} \leftrightarrow (\Lambda^0+H^3) \rightarrow H^3+p+\pi^-+Q_b$,

(c) $He^{4*} \leftrightarrow (\Lambda^0+He^3) \rightarrow He^3+p+\pi^-+Q_c$,

(d) $He^{5*} \leftrightarrow (\Lambda^0+He^4) \rightarrow He^4+p+\pi^-+Q_d$.

The Q-values computed for these cases are $Q_a = 42.8_{-3.8}^{+4.3}$ Mev, $Q_b = 53.4_{-6.2}^{+6.6}$ Mev, $Q_C = 38.9_{-3.4}^{+3.7}$ Mev, $Q_d = 44.0_{-4.6}^{+5.7}$ Mev. If the proton and π meson are regarded as the decay products of a particle residing in the fragment, we may derive the binding energy of the Λ^0 within the fragment by subtracting the above Q-values from the 37.0-Mev Q-value of Λ^0 decay. We thus obtain the Λ^0 binding energies (q) for the four cases: $q_a = -5.9_{-4.3}^{+3.8}$ Mev, $q_b = -16.4_{-6.6}^{+6.2}$ Mev, $q_c = -1.9_{-3.7}^{+3.4}$ Mev, $q_d = -7.0_{-5.7}^{+4.6}$ Mev.

Only in case (c) could the Λ^0 have a positive binding energy within the stated errors of measurement.

If we assume that neutrons are among the secondaries, the Λ^0 binding energy will, of course, be even smaller. Since momentum balance is possible without assuming neutral secondaries, we conclude that the decay is probably of type (c), and the binding energy of the Λ^0 to He^3 is probably less than 2 Mev.

TABLE III. The required ionization corresponding to various assumptions for the secondary fragment (track D, Fig. 1). The ionization of the secondary fragment is estimated to be between 15 and 30 times minimum.

Assumed secondary fragment	Corresponding momentum Mev/c	Required ionization times minimum	Interpretation based on ionization estimate
H^1	445±62	3.4−4.8	Excluded
H^2	445±69	9.2−15	Unlikely
H^3	445±81	17 −28	Possible
He^3	890±131	21 −41	Possible
He^4	890±138	37 −62	Unlikely
Li^6	1335±207	56 −93	Excluded

Many examples of bound Λ^0 decay have been found in nuclear emulsions.[1–18] The fragments involved have charges from 1 to 9e, and they may decay with or without the emission of a π meson. In two events,[7,11] neither a π meson nor an unattached nucleon was emitted. However, in all but two unusual cases,[14,15] the excited particle could be a Λ^0.

Hill[6] and associates at Brookhaven observed (c) in nuclear emulsions. They found a Λ^0 binding energy q_c of $\sim$3 Mev. Naugle *et al.*,[11] also probably observed (c) and obtained $q_c = 2.8\pm1.4$ Mev/c using 37.0 ± 0.5 Mev for the Q-value of Λ^0 decay.

The long lifetime of these events is thought to be due to the slow decay of a single particle, usually a Λ^0, which contains all of the excitation energy of the fragment. Previously it has been possible to set only a lower limit to the lifetime. If our interpretation is correct, the lifetime of the excited He^4 was $(5.4\pm0.6)\times10^{-10}$ sec in this single example.

An interesting characteristic of the present event is the high fragment momentum, which is 1600±300 Mev/c when extrapolated back to the origin of the penetrating shower. In nuclear emulsion events, the excited fragments observed have had ranges that correspond to much smaller momenta.

[1] M. Danysz and J. Pniewski, Phil. Mag. **44**, 348 (1953).
[2] Tidman, Davis, Herz, and Tennent, Phil. Mag. **44**, 350 (1953).
[3] J. Crussard and D. Morellet, compt. rend. **236**, 64 (1953).
[4] Lovera, Silva, Bonacini, DePietri, Fedeli and Roveri, Nuovo cimento **10**, 986 (1953).
[5] Frier, Anderson, and Naugle, Phys. Rev. **94**, 677 (1954).
[6] Hill, Salant, Widgoff, Osborne, Pevsner, Ritson, Crussard, and Walker, Phys. Rev. **94**, 797(A) (1954).
[7] Bonetti, Levi Setti, Pavetti, Searsi, Tomasini, Nuovo cimento **11**, 210 (1954).
[8] Bonetti, Levi Setti, Pavetti, Searsi, Tomasini, Nuovo cimento **11**, 330 (1954).
[9] W. F. Fry and G. R. White, Nuovo cimento **11**, 551 (1954).
[10] P. H. Barrett, Phys. Rev. **94**, 1328 (1954).
[11] Naugle, Ney, Freier, and Cheston, Phys. Rev. **96**, 1383 (1954).
[12] A. Solheim and S. O. Sorensen, Phil. Mag. **45**, 1283 (1954).
[13] Lal, Pal, and Peters, Phys. Rev. **92**, 438 (1953).
[14] W. F. Fry and M. S. Swami, Phys. Rev. **96**, 809 (1954).
[15] Fry, Schneps, and Swami, Phys. Rev, **97**, 1189 (1955).
[16] H. Yagoda, Phys. Rev. **98**, 153 (1955).
[17] Debenedetti, Garelli, Lovera, Tallone, and Vigone, Nuovo cimento **12**, 466 (1954).
[18] B. Waldeskog, Arkiv. Fysik. **8**, 369 (1954).

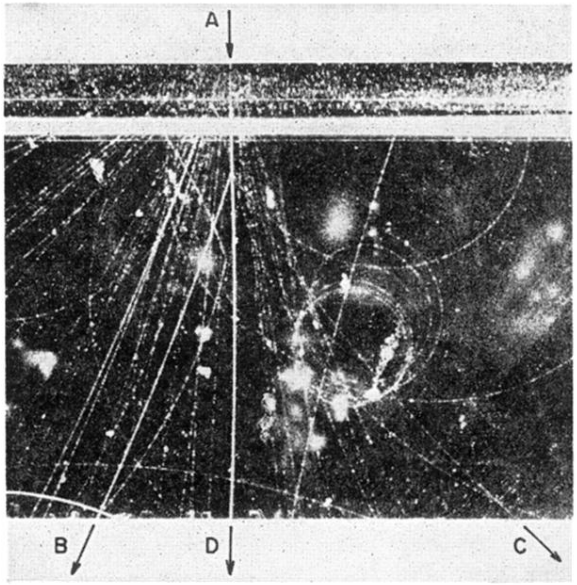

FIG. 1. A cloud-chamber photograph of a delayed fragment decay. A heavy fragment (A) is ejected from a well-defined shower origin 5 mm above the sensitive region of the chamber. The fragment subsequently decays into a proton (B), a light particle consistent with a π^- meson (C), and another secondary fragment (D). The event is consistent with the in flight decay of an excited He^4 nucleus containing a Λ^0 particle. An unrelated $\pi \rightarrow \mu + \nu$ decay appears slightly to the left of track (D).